JOURNAL OF MATERIALS SCIENCE 3 (1968) 33–40

# An X-ray Diffraction Topographic Study of Single Crystals of Melt-Grown Yttrium Aluminium Garnet

J. BASTERFIELD, M. J. PRESCOTT
*Mullard Research Laboratories, Redhill, Surrey, UK*

B. COCKAYNE
*Ministry of Technology, Royal Radar Establishment, St Andrews Road, Great Malvern, Worcs, UK*

*Received 3 August 1967*

Melt-grown crystals of yttrium aluminium garnet usually exhibit an optically imperfect central core region associated with the formation of facets on the solid/liquid interface during growth. The nature of the optical inhomogeneity of the core region, and the general defect structure of the crystals, was investigated by the technique of X-ray diffraction topography. The core region, which showed an elastic strain effect, contained straight growth striations reflecting the development of facets. Comparison was made between undoped and neodymium-doped crystals, and between crystals grown on <111> and <110> growth axes. Impurity striations were thought to be caused by temperature oscillations in the melt ahead of the growing interface. Dislocations, which were observed in the outer regions of the crystals, were sometimes nucleated at inclusions.

## 1. Introduction

Neodymium-doped yttrium aluminium garnet single crystals grown by the vertical-pulling technique are widely used as solid-state lasers. In previous papers [2, 3], several defects which impair the optical perfection of such material have been identified. These include cracks arising from thermal stresses and, in the presence of a doping element such as neodymium, defects arising from local changes in chemical composition due to constitutional supercooling. This latter effect also leads to cavity formation within the crystals. The formation of all these defects can be avoided by suitable control of the growth process. For instance, thermal stresses can be reduced below the yield value by the use of afterheaters, and constitutional supercooling effects can be eliminated by lowering the growth rate. Crystals of yttrium aluminium garnet grown under optimum conditions in order to avoid these defects do, however, exhibit an elastic strain effect in their central core which is associated with the formation of facets on the solid/liquid interface during growth. Because of this optically imperfect core region, laser crystals can only be cut from the outer regions of the crystal. The present paper describes how X-ray diffraction topography has been used to investigate the nature of the optical inhomogeneity of the core region, in addition to the general defect structure of the crystals.

The crystal structure of yttrium aluminium garnet, $Y_3Al_5O_{12}$, cubic space group *Ia3d*, has been described by Yoder and Keith [1]. The unit cell has a lattice parameter of 12.01 Å and contains 160 atoms. No simple close-packed planes are present in the structure.

## 2. Experimental Details

The yttrium aluminium garnet crystals were grown by the vertical-pulling technique [4]. The starting materials were the component oxides, $Y_2O_3$ and $Al_2O_3$, in powder form. In the doped crystals neodymium, and in some cases chromium, were mixed with the component powders in the respective forms of

TABLE I Mass spectrographic analysis of starting materials, showing all impurities present in quantities greater than 1 ppm, expressed in ppm.

| Impurity element | $Al_2O_3$ | $Y_2O_3$ | $Cr_2O_3$ | $Nd_2O_3$ |
|---|---|---|---|---|
| Na | 1.5 | 20 | 30 | 60 |
| Si | 9 | 10 | 40 | — |
| Cl | 160 | 9 | 60 | 380 |
| K | 3 | 4 | 5 | — |
| Ca | — | 8 | 15 | — |
| Mn | — | — | — | 3.5 |
| Fe | — | — | 15 | — |
| Zn | 2 | — | — | — |
| Ga | 2.5 | — | — | — |
| In | 35 | — | — | — |
| W | — | 1.5 | — | — |
| Sm | — | 14 | — | — |
| Dy | — | — | — | 1200 |
| Ho | — | — | — | 130 |
| Yb | 20 | — | — | 485 |

$Nd_2O_3$ and $Cr_2O_3$, prior to melting. A mass spectrographic analysis of the starting materials giving all impurities present in quantities greater than 1 ppm is presented in table I.

The technique of X-ray diffraction topography developed by Lang [5] has now been applied for the first time to single crystals of yttrium aluminium garnet. Crystals having growth axes lying approximately along <110> or<111> directions were studied. Crystal sections were cut perpendicular to the growth axes, and prepared as wafers approximately 50 $\mu$m thick by chemical polishing in orthophosphoric acid at 280° C. The topographs were recorded on Ilford nuclear plates, type L4, with 100 $\mu$m thick emulsion; Ag K$\alpha$ radiation was used throughout. Typical exposure times were of the order of 30 h for a 1 cm diameter crystal.

It should be noted that all topographs were 402 or 422 type reflections. These correspond on the stereographic projections which follow with the poles of the crystal planes {201} and {211} respectively.

## 3. Core Region of Crystals

### 3.1. Undoped Crystals

A composite photograph of a topograph of an undoped <110> axis crystal is shown in fig. 1a. The centre of the crystal shows a pattern of striations similar to the impurity striations widely observed in vertically-pulled single crystals [6]. Knowing the orientation of the crystal the orientation of the planes associated with the striations may be determined crystallographically as follows. The traces of the striations on the topograph are plotted on a stereogram (for the reflecting planes used, the distortion of the true angles in the crystal by the

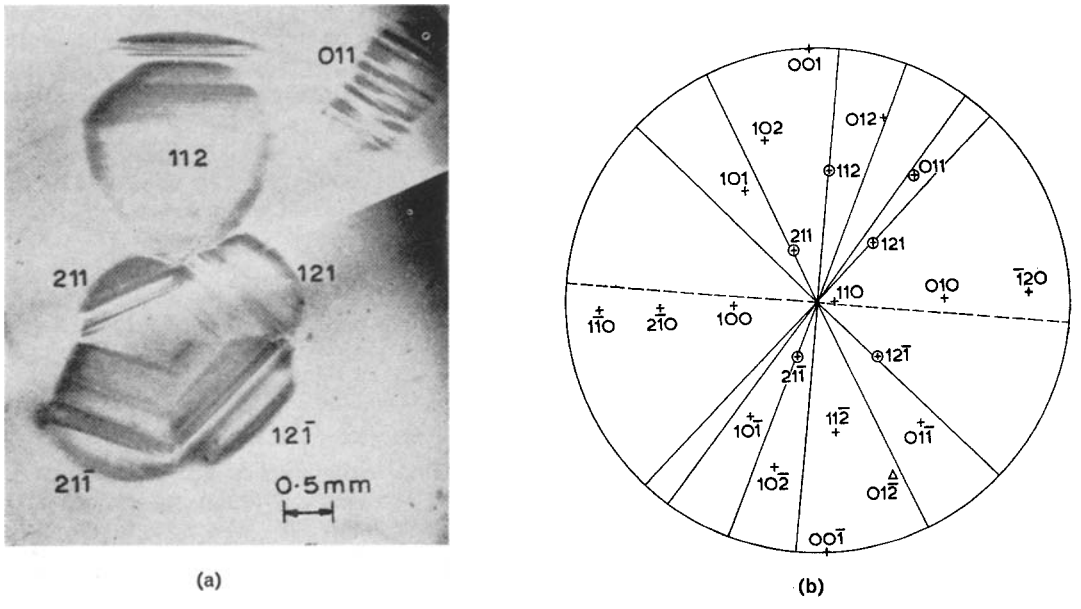


(a) (b)

*Figure 1* (a) X-ray topograph, 024 reflection, of core region of undoped $Y_3Al_5O_{12}$, <110> growth axis. (b) Orientation of facets determined from (a). △ denotes Bragg reflection; ○ denotes poles of planes on which faceting occurred.

geometric arrangement of X-ray beam, crystal, and film is small, and can be ignored). The poles of the crystallographic planes, along which the striations form, lie somewhere along the great circles constructed at right angles to the traces. By analogy with single crystals of flux-grown garnets, which are bounded by crystallographic faces of the forms {110} and {211}, only the above low-index planes are considered, and a consistent interpretation emerges. The stereogram in fig. 1b shows the traces of the striations as broken lines, while the full lines represent the great circles along which the poles of the striation-forming planes must lie. Only one broken line is shown, that corresponding to the (112) plane, to avoid overcrowding the stereogram with a large number of lines. Comparing figs. 1a and 1b, the striations are seen to be consistent with the (211), (121), (12$\bar{1}$), (21$\bar{1}$), (112), and (011) planes.

The same crystal was also examined with plane-polarised light. Although the striated areas observed in the topograph could be seen to be optically imperfect, striations were only resolved on the (121), (12$\bar{1}$), and (011) planes. The contrast, arising from stress birefringence, was much poorer than that obtained in the X-ray diffraction topographs, and only the latter technique was used to examine the remaining crystals.

A feature of the striations shown in fig. 1a is the variation in contrast along them. Usually stronger contrast is shown at the ends of the striations. This is shown particularly by the (011) and (121) planes in fig. 1a and also in later topographs, e.g. fig. 3.

Crystals have also been grown on a <111> growth axis, and an X-ray diffraction topograph of a $\bar{2}40$ reflection of an undoped yttrium aluminium garnet crystal is shown in fig. 2a. The core region of the crystal was less defective than in the <110> growth axis crystals, and showed only a few striations. Fig. 2b shows that the crystal plane giving rise to these was the (121). The other two {211} planes of the group which might have shown faceting did not exhibit striations, but the appearance of the core region indicated that it was still stressed with respect of the outer regions of the crystal, and that faceting was present. The striations were postulated to occur on the (121) plane rather than the (101) plane, for reasons described later in a description of the doped crystal having a <111> growth axis. The position of the three v-shaped areas in fig. 2a was consistent with faceting occurring on the (121), (112) and (211) planes, and on the (101), (011) and (110) planes. The v-shaped areas may then be interpreted as the boundaries between the {211} and {110} facets.

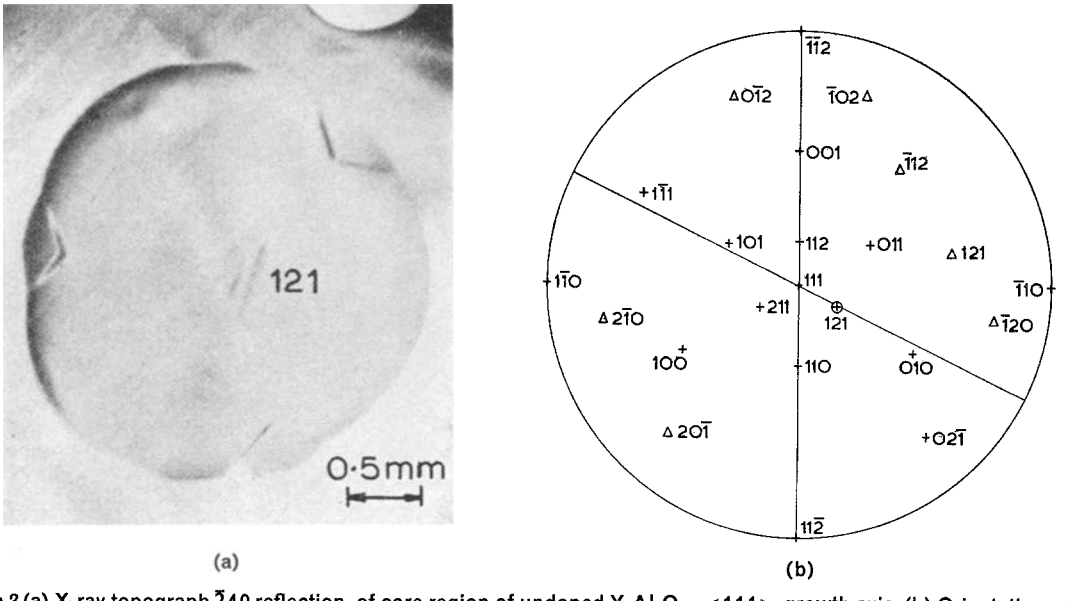


*Figure 2* (a) X-ray topograph $\bar{2}40$ reflection, of core region of undoped $Y_3Al_5O_{12}$, <111> growth axis. (b) Orientation of facets determined from (a). △ denotes Bragg reflections; ○ denotes poles of plane on which faceting occurred.

Undoped crystals of yttrium aluminium garnet were annealed in air at 1800° C for 24 and 48 h. X-ray diffraction topographs showed that neither the curved striations in the outer regions of the crystals (see section 4), nor those associated with faceting in the core, were removed by the annealing treatment. A possible reduction in the sharpness of the diffraction contrast indicated that some slight modification of the striations may have taken place.

### 3.2. Doped Crystals

The X-ray diffraction topograph of a <110> axis crystal doped with 0.2 at. % neodymium (fig. 3) may be compared with that of the undoped crystal shown in fig. 1a (the circular white areas are holes produced during chemical polishing). The poles of the crystal planes responsible for the striations have been determined as before, by means of a stereogram.

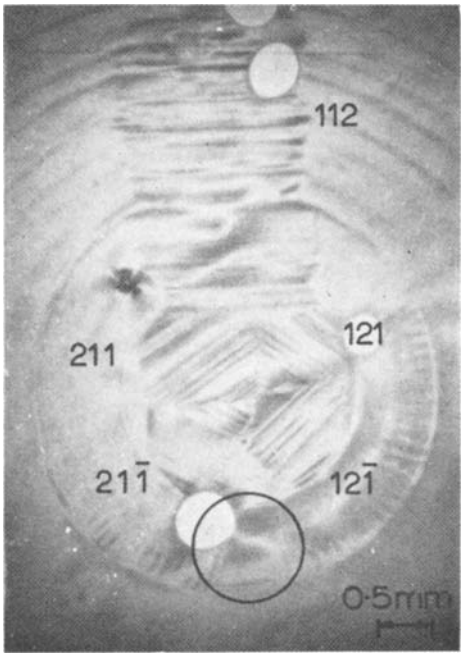


*Figure 3* X-ray topograph, $20\bar{4}$ reflection, of core region of 0.2 at. % Nd-doped $Y_3Al_5O_{12}$, <110> growth axis.

With the exception of the (011) plane, faceting has occurred on the same group of planes as before, that is the (211), (121), (12$\bar{1}$), (21$\bar{1}$) and (112) planes. The irregular nature of the diffraction contrast associated with the striations is apparent, particularly on the (112) and (121) planes. In general appearance the striations are broader and more diffuse than in the undoped crystals. An inclusion in the crystal is also shown by the topograph.

The most significant difference observed is the radial striations found in the doped crystal, and shown in fig. 3 at the edge of the central faceted area. They may be compared with the cracking, previously reported by Cockayne [2], in neodymium-doped yttrium aluminium garnet crystals, which occurs in a similar area of the crystal. The tendency to crack was found to be markedly dependent upon the amount of neodymium incorporated in the crystal, and consequently it seems likely that the radial striations are associated with strain due to enhanced neodymium incorporation in the crystal. This view is supported by radioactive tracer experiments carried out in the present work, which show that the ratio of neodymium incorporated into the central faceted regions to that incorporated in the bulk of the crystal is 1.2:1; $^{147}Nd$ was used as the tracing isotope.

The X-ray diffraction topograph of a <111> axis crystal doped with 0.6 at. % Nd (fig. 4) shows striations in the central facets, similar to those in the neodymium-doped <110> axis crystal. The radial striations are, however, not present in this case, but the general level of defects is much greater than in the corresponding undoped crystal (fig. 2a). The facets were considerably more pronounced in the neodymium-doped crystal than in the undoped one, and the directions of the growth striations confirmed

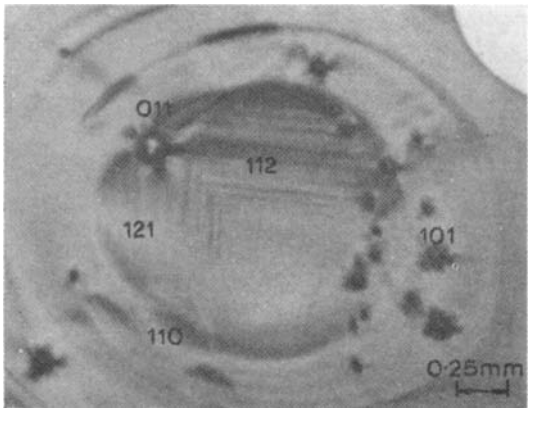


*Figure 4* X-ray topograph, $\bar{2}40$ reflection, of core region of 0.6 at. % Nd-doped $Y_3Al_5O_{12}$, <111> growth axis.

that faceting had occurred on the {1 1 0} planes as well as the {2 1 1} planes.

The addition of 0.2 at. % chromium to a <1 1 1> axis crystal doped with 0.2 at. % neodymium appears to relieve much of the strain which is introduced in the core region by the neodymium alone. Radioactive tracer experiments using $^{51}Cr$ have shown that chromium segregates more uniformly than neodymium across the crystal, the ratio of chromium on the central facets to that in the bulk crystal being 0.95 :1.

The main features of the core region of such a crystal are shown in the topograph of fig. 5a.

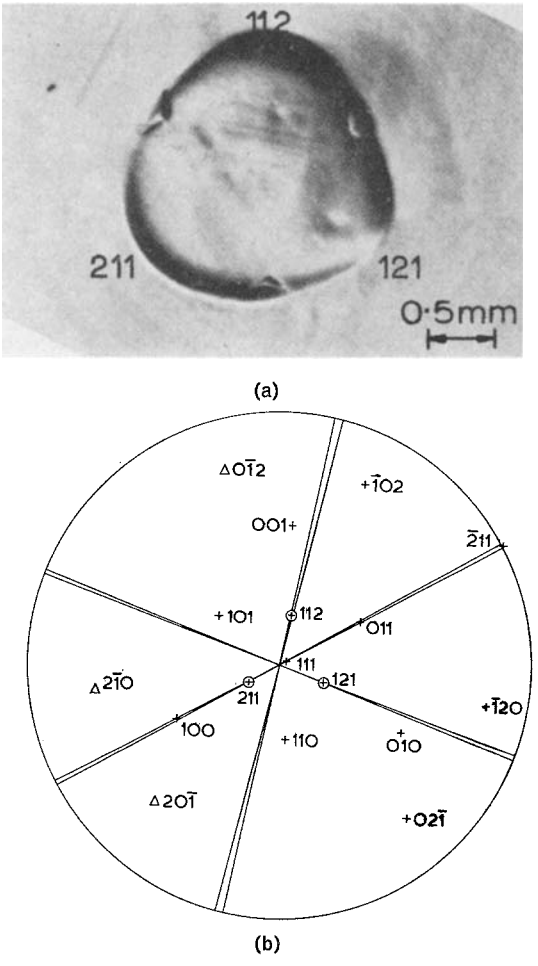


*Figure 5* (a) X-ray topograph, 40$\bar{2}$ reflection, of core region of 0.2 at. % Nd, 0.2 at. % Cr-doped $Y_3Al_5O_{12}$, <1 1 1> growth axis. (b) Orientation of facets determined from (a) and 0$\bar{2}$4 and 4$\bar{2}$0 reflections. △ denotes Bragg reflections; ○ denotes poles of planes on which faceting occurred.

The growth pattern is substantially the same as the undoped crystal, but striations are more pronounced, and may be detected on the (2 1 1) and (1 1 2) planes. Using other Bragg reflections, striations were also detected on the (1 2 1) plane (fig. 5b). Three v-shaped areas were again observed, and faceting is thought to have occurred to a small degree on the three neighbouring {1 1 0} planes, although no striations were detected.

It is instructive at this stage to compare the stereograms of figs. 2b and 5b. In fig. 2b we cannot differentiate between striations occurring on the (1 2 1) and (1 0 1) planes, since the striations on both will be parallel if the normal to the slice is aligned exactly along the [1 1 1] direction. This corresponds to the case for the undoped crystal. However, the [1 1 1] axis of the doped crystal is tilted 4° towards the [$\bar{2}$ 1 1] direction and this allows us to differentiate between striations on the {2 1 1} and {0 1 1} planes in fig. 5b. Alternatively, by comparing the crystal and stereogram, and noting on which side of the stereogram the striations occur, we could make the choice unambiguously with an exactly oriented crystal, since the crystal-melt interface composed by the facets is always convex towards the melt. However in this case it is essential to know the sign of the direction of pulling in the crystal slice. The two alternatives are shown in fig. 6 and the orientation of viewing direction and pulling direction depicted in fig. 6b is chosen for correct comparison with the stereogram.

## 4. Outer Region of Crystals

In general, the outer region of the crystals was considerably more perfect than the core region. Usually when striations were observed, they were curved as shown in figs. 3 and 7, indicating the existence of a curved interface during growth. One crystal, however, did show faceting on the (0 1 1) plane towards the edge of the crystal (fig. 1a). The undoped crystals appeared to be more perfect than the doped ones, suggesting that dopant is either incorporated in the striations or is partly a cause of them. Alternatively, since the dopant oxides used were much less pure than the yttrium and aluminium oxides, the striations may also be associated with an increased impurity level.

The doped crystals showed other additional features. The 0.2 at. % neodymium-doped crystal showed striations whose curvature was inverse to those normally appearing. They occur

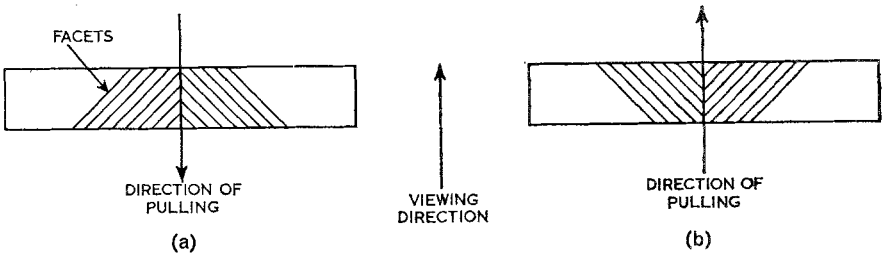


*Figure 6* Sketch showing orientation of facets with respect to viewing direction.

in the original plate of fig. 3 at the position circled, but the contrast is low and may be lost in reproduction. The inverse curvature of the striations is presumably associated with the development of a region of concave solid/liquid interface during crystal growth. Additional inhomogeneities were also detected in the neodymium- and chromium-doped crystal. The outer skin showed short radial striations, and was preferentially attacked by phosphoric acid during polishing. It is thought that a region of pronounced segregation occurred in a thin outer skin of the crystal. Radioactive tracer experiments showed that such a region existed, but the layer was too thin for quantitative data to be obtained. Dislocations and inclusions, which will be discussed separately in a later section, have also been observed.

## 5. Stress Anisotropy Associated with Striations

Because the striations associated with faceting are observed by a diffraction contrast mechanism, it has proved possible to obtain some information on the strain axis, which is approximately uniaxial, associated with the striations. The undoped crystal of yttrium aluminium garnet grown on a <111> axis was examined first, and table II shows the relative visibility of the striations contained in this crystal, for the topographs taken, using different Bragg reflections. Zero visibility should be observed when the strain axis lies within the Bragg reflecting plane. Hence, if two reflections are obtained exhibiting zero visibility, the strain axis may be readily found using a stereogram. As shown in fig. 2a and table II, striations are visible in the $\bar{2}40$ reflection. Zero visibility of the striations is obtained in $\bar{2}04$ and $40\bar{2}$ reflections, and near zero visibility is obtained in the $4\bar{2}0$ and $0\bar{2}4$ reflections. These results indicate strain axes along either the [010] or [121] directions, but it does not appear possible to decide with certainty between the two. The visibility criterion may be affected by the presence of fine-scale inclusions or precipitates localised in the striations.

TABLE II Relative visibility of the striations contained in undoped <111>, yttrium aluminium garnet crystal, for the topographs taken, using different Bragg reflections.

| Specimen | Growth striations on (hkl) plane | Reflection | Contrast |
|---|---|---|---|
| Undoped <111> growth axis | 121 | $\bar{2}40$ | medium |
| | | $\bar{2}42$ | weak |
| | | $\bar{2}24$ | weak |
| | | $\bar{2}04$ | invisible |
| | | $40\bar{2}$ | invisible |
| | | $4\bar{2}0$ | very weak |
| | | $0\bar{2}4$ | very weak |

Growth striations in yttrium aluminium garnet may also be observed in a polarising microscope by their stress birefringence patterns. The directions of the principal stresses set up by the striations may be determined from the positions of extinction, when the crystal slice is rotated relative to the crossed polarisers. Several crystal slices exhibiting growth striations were examined. These included the core region of longitudinal sections of melt-grown yttrium aluminium garnet crystals having <111> growth axes, and flux-grown yttrium aluminium garnet and yttrium gallium garnet crystals. In each case the bands exhibited extinction when their direction lay within a few degrees of that of the polariser or analyser. Hence the birefringence results are compatible with a strain axis perpendicular to the striations, that is, with a [121] strain axis in the case previously considered.

## 6. Dislocations and Inclusions

In general the crystals contained few dislocations or inclusions. Among those examined, one of the worst affected was the 0.2 at. % neodymium-doped crystal, which contained

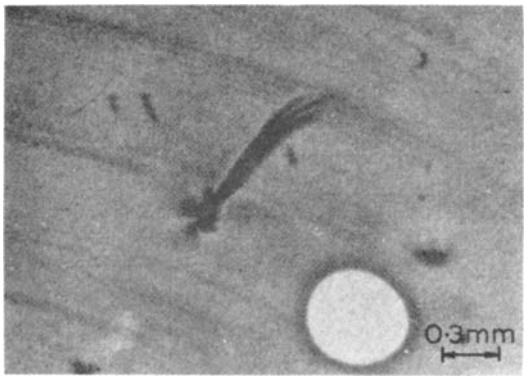


*Figure 7* X-ray topograph of outer region of 0.2 at. % Nd-doped $Y_3Al_5O_{12}$ showing curved striations and the nucleation of dislocations at an inclusion.

several examples of dislocations probably nucleated at inclusions, one such example being shown in fig. 7. Most of the dislocations lay at large angles to the crystal slice, making the determination of the Burgers vector difficult, and attention was concentrated on those dislocations lying more nearly in the plane of the slice. These often radiated from inclusions in the crystal. One of the dislocations was made to disappear in topographs taken using the $\bar{2}40$ and $42\bar{0}$ reflections. Using the invisibility criterion, $g.b = 0$, where $g$ is the diffraction vector, and $b$ the Burgers vector of the dislocation, a Burgers vector of $a[100]$ was obtained (in the [100] direction this is the shortest lattice vector). With such a large Burgers vector, approximately 12.01 Å, one might expect to find hollow dislocations in garnet crystals [8], and this phenomenon has often been observed in crystals of yttrium gallium garnet grown from a PbO/PbF flux [7]. It has not proved possible to get an unambiguous determination of the Burgers vector of the longest dislocations in the slice. It is probable that the dislocations nucleated at inclusions are decorated with impurities from the melt and that the associated impurities interfere with the invisibility criteria. Such decoration of dislocations has been observed in aluminium, iron and gallium garnets grown by the flux method [7].

## 7. Impurity Striations

The curved and striated strain patterns observed in the outer regions of the doped crystals are consistent with the impurity growth striations already observed in yttrium aluminium garnet single crystals [2]. Such striations delineate the shape of the solid/liquid interface during growth, and the straight striations observed in the central core of the crystals merely reflect the development of flat regions, i.e. facets, on this interface. One of us [6] has recently shown that, in oxide single crystals, such striations arise from temperature oscillations which occur in the melt ahead of the growing interface. Such oscillations cause striations by producing modulations of the growth rate, which in turn modulate the impurity incorporation. As the magnitude of the oscillations is approximately constant across the interface, the enhanced banding observed on the facets is consistent with a higher impurity concentration in the faceted regions, as demonstrated by neodymium, since a given modulation in growth rate will produce a corresponding change in the fractional amount of impurity incorporated ($\Delta c/c$, where $c$ denotes concentration). Thus in the regions where $c$ is greater, i.e. on the facets, $\Delta c$ will be correspondingly greater in order to keep $\Delta c/c$ constant. As the banding is also observed in undoped crystals, again preferentially on the facets, it may be concluded that most of the impurities present in the starting material segregate in a similar manner to neodymium.

It has been shown that impurity banding in oxides can be removed by growing the crystals under very low temperature gradient conditions, when temperature oscillations are very small in magnitude ($< 1°$ C). In the present case, no advantage would be gained by the use of such conditions, as steep temperature gradients are required to restrict the size of the central strained regions, and to prevent the formation of defects due to constitutional supercooling. Both of these defects are more detrimental to the optical perfection and laser performance of the crystals than impurity banding.

## 8. Conclusions

Striations associated with planar regions on the solid/liquid interface, i.e. facets, have been observed by X-ray diffraction topography in Czochralski-grown single crystals of yttrium aluminium garnet. From the morphology of the striations, faceting was found to occur on {211} and {110} planes. An increased yield of good material was obtained from crystals grown on a <111> growth axis, because the cross-sectional area of crystal subject to faceting appeared consistently smaller than for the

crystals grown with a <110> growth axis. The striations could not be removed by short term annealing at 1800° C.

## Acknowledgements

The authors wish to thank Mr A. E. Jenkinson (MRL) for help and advice on X-ray diffraction topography, Mr M. P. Gates (RRE) for his assistance during crystal growth, and Mr O. Jones (RRE) for his advice on the radioactive tracer work.

## References

1. H. S. YODER and M. L. KEITH, *Amer. Min.* **36** (1951) 519.
2. B. COCKAYNE, *Phil Mag.* **12** (1965) 943.
3. W. BARDSLEY and B. COCKAYNE, *Crystal Growth* (supplement to *J. Phys. Chem. Sol.*) (1967) 109.
4. B. COCKAYNE, D. S. ROBERTSON, and W. BARDSLEY, *Brit. J. Appl. Phys.* **15** (1964) 1165.
5. A. R. LANG, *Acta Cryst.* **12** (1959) 249.
6. B. COCKAYNE and M. P. GATES, *J. Matls. Sci.* **2** (1967) 118.
7. M. J. PRESCOTT and J. BASTERFIELD, to be published.
8. F. C. FRANK, *Acta Cryst.* **4** (1951) 497.